Leukemia
https://doi.org/10.1038/s41375-020-0709-0

ARTICLE

Stem cell transplantation

Targeting NAD immunometabolism limits severe graft-versus-host disease and has potent antileukemic activity

Romana R. Gerner[1,2,8] · Sophie Macheiner[1,2] · Simon Reider[2] · Kerstin Siegmund[3] · Felix Grabherr[1] · Lisa Mayr[1] · Bernhard Texler[2] · Patrizia Moser[4] · Maria Effenberger[1] · Hubert Schwaighofer[1] · Alexander R. Moschen[1,2] · Brigitte Kircher[5] · Herbert Oberacher[6] · Robert Zeiser[7] · Herbert Tilg[1] · David Nachbaur[5]

Received: 2 June 2019 / Revised: 6 December 2019 / Accepted: 14 January 2020

Abstract

Acute graft-versus-host disease (aGVHD) and tumor relapse remain major complications after allogeneic hematopoietic stem cell transplantation. Alloreactive T cells and cancer cells share a similar metabolic phenotype to meet the bioenergetic demands necessary for cellular proliferation and effector functions. Nicotinamide adenine dinucleotide (NAD) is an essential co-factor in energy metabolism and is constantly replenished by nicotinamide phosphoribosyl-transferase (Nampt), the rate-limiting enzyme in the NAD *salvage pathway*. Here we show, that Nampt blockage strongly ameliorates aGVHD and limits leukemic expansion. Nampt was highly elevated in serum of patients with gastrointestinal GVHD and was particularly abundant in human and mouse intestinal T cells. Therapeutic application of the Nampt small-molecule inhibitor, Fk866, strongly attenuated experimental GVHD and caused NAD depletion in T-cell subsets, which displayed differential susceptibility to NAD shortage. Fk866 robustly inhibited expansion of alloreactive but not memory T cells and promoted FoxP3-mediated lineage stability in regulatory T cells. Furthermore, Fk866 strongly reduced the tumor burden in mouse leukemia and graft-versus-leukemia models. Ex vivo studies using lymphocytes from GVHD patients demonstrated potent antiproliferative properties of Fk866, suggesting potential clinical utility. Thus, targeting NAD immunometabolism represents a novel approach to selectively inhibit alloreactive T cells during aGVHD with additional antileukemic efficacy.

Introduction

Cellular (energy) metabolism plays a crucial role in immune cell fate, regulation, and function [1]. Upon activation, T lymphocytes, as sentinels of the adaptive immune system, undergo a profound metabolic reprogramming to meet the increased bioenergetic demands for transition from quiescent to effector T cells (Teff) [2]. While the minimal

These authors contributed equally: Romana R. Gerner, Sophie Macheiner

These authors contributed equally: Herbert Tilg, David Nachbaur

Supplementary information The online version of this article (https://doi.org/10.1038/s41375-020-0709-0) contains supplementary material, which is available to authorized users.

✉ Romana R. Gerner
romana.gerner@i-med.ac.at

✉ David Nachbaur
david.nachbaur@i-med.ac.at

[1] Department of Internal Medicine I, Gastroenterology, Hepatology & Endocrinology, Medical University Innsbruck, Innsbruck, Austria

[2] Christian Doppler Laboratory for Mucosal Immunology, Medical University Innsbruck, Innsbruck, Austria

[3] Department for Pharmacology and Genetics, Medical University Innsbruck, Innsbruck, Austria

[4] Department of Pathology, Medical University Innsbruck, Innsbruck, Austria

[5] Department of Internal Medicine V, Hematology & Oncology, Medical University Innsbruck, Innsbruck, Austria

[6] Institute of Legal Medicine and Core Facility Metabolomics, Medical University Innsbruck, Innsbruck, Austria

[7] Department of Hematology, Oncology and Stem Cell Transplantation, Freiburg University Medical Center, Albert–Ludwigs–University, Freiburg, Germany

[8] Present address: Division of Host–Microbe Systems and Therapeutics, Department of Pediatrics, University of California San Diego, 92037 La Jolla, CA, USA

Published online: 23 January 2020

biosynthetic requirements of naive T cells are mainly supplied by mitochondrial respiration, activated T cells strongly rely on additional energy sources such as aerobic glycolysis, similar to metabolism in cancer cells [3]. Nicotinamide adenine dinucleotide (NAD) is a central metabolic co-factor and redox carrier in these ATP-generating pathways and beyond serves as substrate for NAD-catabolic enzymes including mono- or poly-ADP-ribose polymerases and sirtuins. The latter are implicated in a wide range of biological processes such as energy sensing, DNA repair, cell cycle regulation, and immune modulation [4, 5]. Accordingly, NAD indirectly regulates a plethora of metabolic pathways and its availability is determined by the relative rates of biosynthesis and degradation. In mammals, the enzyme nicotinamide phosphoribosyl-transferase (Nampt) catalyzes the rate-limiting step of the NAD *salvage pathway* and thereby prevents intracellular NAD shortage [6]. In addition to its enzymatic function, proangiogenic and cytokine-like roles have been attributed to secreted/extracellular Nampt, primarily by enhancing cell survival, effector functions of antigen-presenting cells and promoting alloantigen-driven lymphocyte proliferation [7, 8]. However, despite the vital necessity of Nampt, its upregulation has been linked to various inflammatory and metabolic disorders including cancer in mice and men, and further underpins Nampt's role in energy metabolism, immune processes, and malignancy [7, 9–11]. Fk866, a potent small-molecule inhibitor of intracellular Nampt, was initially discovered in search of novel anticancer substances, but additionally has been proven beneficial in inflammatory and malignant diseases including hematologic neoplasia [12–14].

Acute graft-versus-host disease (aGVHD), the major complication of allogeneic hematopoietic stem cell transplantation (allo−HSCT), displays a multiorgan inflammatory syndrome par excellence. Alloantigen-activated donor T cells generate robust immune responses resulting in tissue damage of skin, liver, and gut [15]. Gastrointestinal (GI) involvement is particularly relevant for perpetuating systemic GVHD, as intestinal damage increases gut permeability and thereby encourages the translocation of bacteria and proinflammatory stimuli [16]. While corticosteroids remain the primary treatment for aGVHD, a substantial proportion of patients is refractory and requires further treatment [17, 18]. Steroid-refractory aGVHD and severe GI-manifestations are associated with high morbidity and mortality, implying that novel therapeutic approaches are strongly required [19].

Previous studies emphasized, that alloreactive T lymphocytes critically upregulate the metabolic machinery in the context of aGVHD. Moreover, Nampt is induced upon mitogenic and allogeneic activation of T cells [20–22]. Here, we show that Nampt is strongly expressed in intestinal T cells during human and mouse aGVHD, which further provided a rationale to target alloreactive T cells by Fk866 in experimental GVHD. Nampt and the NAD metabolism were essential for proliferating Teff but not for regulatory or memory T cells, which displayed highly differential susceptibility to Fk866-mediated NAD depletion. Fk866 treatment resulted in strongly reduced severity of experimental GVHD and, besides its immune modulatory effects, was accompanied by a marked antitumor efficacy in mouse graft-versus-leukemia (GVL) models. Our preclinical data were supported by human ex vivo studies, suggesting that manipulating the bioenergetics of T-cell subsets by Fk866 may provide a novel strategy to treat GVHD and further eradicate residual malignant cells.

Materials and methods

A detailed description of cell culture experiments and reagents is provided as part of the Supplementary methods. Antibodies are listed in Supplemental Table 1.

Patients and samples

Consecutive patients undergoing allo-HSCT at our institution due to malignant hematological diseases were included after written informed consent was obtained. The study was approved by the local ethics committee. Patients received myeloablative conditioning followed by HLA-matched related or unrelated HSCT. Cyclosporine A (CsA) and methotrexate or mycophenolate mofetil were administered for GVHD prophylaxis according to Seattle protocols [23, 24]. For serum analysis, heparinized blood samples were collected weekly starting 7−2 days (d) prior to conditioning until d +70 after allo-HSCT and stored at −80 until assaying. Sera from healthy volunteers were used for NAMPT baseline quantification by ELISA (detailed protocol is described in Supplementary methods). Acute GVHD was diagnosed from clinical symptoms and/or gut biopsies and classified according to revised Seattle criteria [25].

Mice and animal husbandry

C57BL/6 (B6, H−2K^{b}) and BALB/c (H−2K^{d}) mice were purchased from Charles River and were bred and maintained under specific pathogen-free conditions at the animal facility of the Medical University Innsbruck in accordance with Institutional Animal Care and Use of Committee regulations. All experiments were approved by the Austrian Ministry of Science and Research.

GVHD model and Fk866 treatment

Bone marrow transplantation (BMT) was performed as previously described [26]. Briefly, 10 to 12−week old,

female recipients were subjected to either 8 Gy (BALB/c) or 11 Gy (B6) total body irradiation (TBI) from a gamma irradiation source on d −1. Bone marrow from male C57BL/6 or BALB/c donors was harvested aseptically from femurs and tibias followed by T-cell depletion (TCD) using anti-CD90.2 microbeads with a MACS cell separation system. Splenic T cells from the same mice were enriched using a Pan T cell isolation kit (both Miltenyi, Bergisch Gladbach, Germany). On d 0, recipients were intravenously injected with 5×10^6 syngeneic or allogeneic TCD−BM cells along with $0.5-1 \times 10^6$ T cells in allogeneic settings. Mice were administered 6 mg/kg bodyweight (bw) Fk866 dissolved in 200 µl PBS (biorbyt, Cambridge, UK) or vehicle control twice daily intraperitoneally (i.p.) from d +5 until the end of experiments. Animals received Trimethoprim/Sulfamethoxazole (Eusaprim, Aspen Pharma, Dublin, Ireland) ad libitum throughout experiments and were monitored for clinical GVHD signs as previously described [27]. Peripheral blood was analyzed by the scil Vet−ABC analyzer (scil animal care company, Viernheim, Germany). Target organs were collected and immediately snap frozen or formalin-fixed at indicated time points. Additional protocols and procedures are described in online Supplementary methods.

Tumor model and in vivo bioluminescence imaging (BLI)

For GVL experiments, we utilized the murine leukemia cell line WEHI-3B (myelomonocytic) or the B cell lymphoma cell line A20 in the B6 → BALB/c setting with minor modifications [28]. A20 *luc* and WEHI-3B *luc* (both H−$2k^d$) were a kind gift of RZ (Freiburg, Germany) and were cultured in RPMI (A20) or IMDM (WEHI) containing 10% FCS/1% Pen/Strep (Fisher Scientific, Vienna, AT). Briefly, BALB/c recipients underwent TBI on d −1 and were administered TCD BM cells from B6 or BALB/c donors together with or without A20 *luc* or WEHI-3B *luc* cells on d0. Allogeneic groups received 0.5×10^6 splenic T cells (B6) isolated as described above 48 h later [29]. Tumor engraftment/proliferation was analyzed by in vivo BLI as previously described using an IVIS2000 charge-coupled device imaging system (Xenogen, Alameda, CA) [30]. Therefore, mice were injected with 10 µg/g bw D-luciferin i.p. (Roth Lactan, Graz, AT) 5 min prior to imaging. Data were analyzed and quantified with Living Image software (Xenogen).

Statistical analysis

Statistical significance was assessed using a two-tailed Student's *t* test. One-way analysis of variance (ANOVA) with Bonferroni's post-hoc test was used for comparisons >2 groups. Non-normally distributed data were analyzed by Mann–Whitney *U* test (two groups) or Kruskal–Wallis test followed by Dunn's multiple comparison test (three or more groups) where appropriate. A p value < 0.05 was considered significant. Data were analyzed and illustrated using GraphPad Prism V.7.0 (GraphPad Software, San Diego, CA).

Results

Nampt is highly upregulated during human and mouse aGVHD

Since severe GVHD displays one of the strongest immune responses in humans, we analyzed NAMPT serum levels in patients with and without acute GI−GVHD over time (patient and transplant characteristics outlined in Supplementary Table 2). Compared with patients that never presented with clinical GVHD, patients with grade II−IV GI−GVHD demonstrated significantly elevated systemic NAMPT levels, starting during the early posttransplant period and constantly increasing over time (Fig. 1a). To determine potential cellular sources of NAMPT, we further performed immunofluorescence on colonic sections from these patients. Various cell types and tissues express low levels of NAMPT at baseline, which was confirmed in patients without GVHD (Fig. 1b). In contrast, NAMPT strongly and predominantly co-localized with $CD3^+$ T cells in patients with confirmed GVHD diagnosis (Fig. 1b and Supplementary Fig. 1). These data led us to investigate the impact of Nampt during the course of experimental aGVHD. B6 mice underwent allo-BMT from BALB/c donors (i.e., major and minor mismatch) and Nampt expression was tracked in colonic donor immune cells by flow cytometry. In accordance with our findings in human intestinal GVHD, Nampt expression was most pronounced in colonic $CD3^+$ T cells and increased over time reaching maximum levels between d +8–12 (Fig. 1c), which coincides with the clinical onset of GVHD in mice and when donor-derived immune cells are already fully present in the intestine (Fig. 1c).

Fk866-mediated Nampt blockage mitigates experimental GVHD

We next investigated the consequence of Nampt blockage by the small-molecule inhibitor Fk866 in fully MHC-mismatched experimental BMT models [12]. Following TBI or BU/CY conditioning, mice were transplanted with syngeneic or allogeneic BM ± T cells and either treated with vehicle or Fk866 in a therapeutic setting (outlined in Fig. 2a and Supplementary Fig. S2A). Because the GVHD onset in mice typically occurs around d +7, Fk866 or vehicle

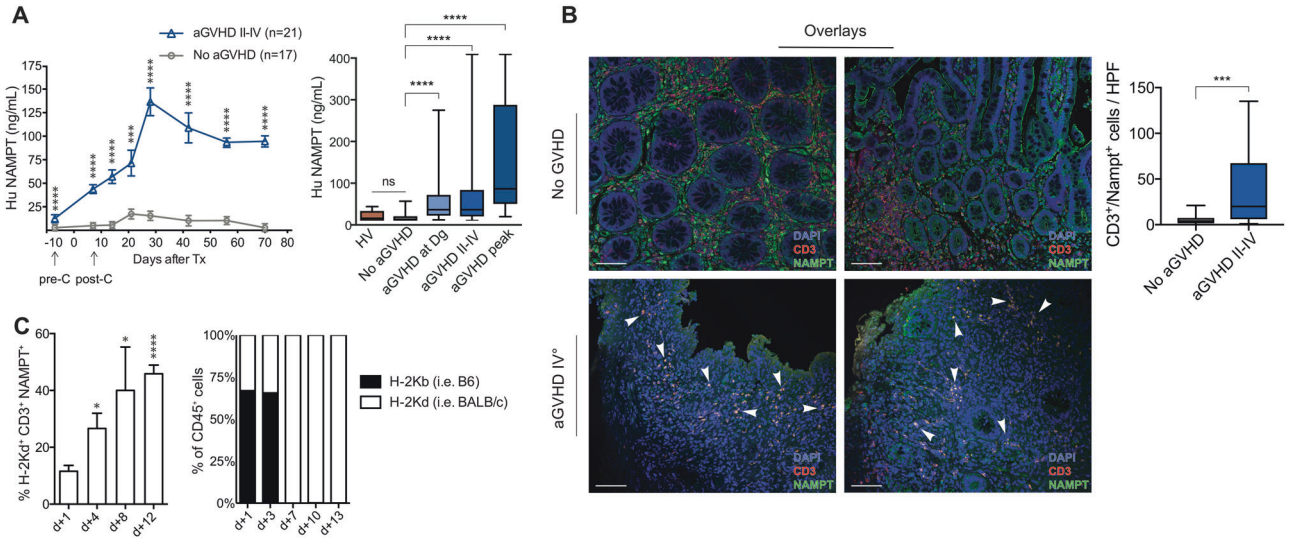

Fig. 1 NAMPT is elevated in patients with acute GI–GVHD and is highly abundant in human and mouse intestinal T cells. a The kinetic profiles of NAMPT in serum from patients with (blue triangles) or without (gray circles) acute GI−GVHD are shown. pre-C = preconditioning week; post-C = postconditioning week. Values are expressed as mean ± SEM. $n = 17$ (no GVHD) or 21 (GI–GVHD). Boxplots represent cumulative values throughout the observation period and are grouped according to occurrence, severity, or peak values. Whiskers plot minimum to maximum values of data with the band inside the box displaying the median. **b** Colonic biopsies from patients at different time points after allo-HSCT were taken to exclude or confirm a clinically suspected diagnosis and were used for immunofluorescence stainings. Human CD3 was detected with AF568, NAMPT was detected with AF488 and DAPI stainings indicate cell nuclei. Images were visualized with confocal microscopy and co-localization of CD3 and NAMPT is indicated by a light–yellow appearance in the merged pictures (some are highlighted by white arrows). Non-merged images and isotype control stainings are shown in Supplementary Figure S1. Representative images of four individual patients are shown. The number of $CD3^+$ $NAMPT^+$ T cells per HPF was enumerated within human intestinal histology sections as detected by immunofluorescence. $n = 17$ (no GVHD) or 21 (GI–GVHD). (×20 magnification, scale bars represent 50 µm). **c** B6 mice underwent TBI and received 5×10^6 TCD BM cells along with 1×10^6 T cells from BALB/c donors (allo). Subsequently, LPMC were isolated at different time points and the presence of donor $CD3^+$ $Nampt^+$ T cells was investigated over time by flow cytometry along with the proportion of cells displaying donor (BALB/c, i.e. H–2 K^d) and recipient (B6, i.e. H–2K^b) MHC haplotypes out of $CD45^+$ cells. $n = 5$/group; two independent experiments. $^*p < 0.05$; $^{**}p < 0.01$; $^{***}p < 0.001$, $^{***}p < 0.0001$; GI−GVHD gastrointestinal graft-versus-host disease, HV healthy volunteer, Dg diagnosis, HPF high power field, TBI total body irradiation, TCD T-cell depletion, BMT bone marrow transplantation, LPMC lamina propria mononuclear cells.

treatment was initiated on d +5, prior to the peak Nampt expression in $CD3^+$ T cells (Fig. 1c). Subsequent to allogeneic BMT, vehicle-treated animals developed severe GVHD reflected by sustained weight loss (Fig. 2a and Supplementary Fig. S2A), increased overall clinical GVHD scores and colonic shortening (as indicator for colonic inflammation; Fig. 2b and Supplementary Fig. S2B). In contrast, Fk866-treated mice were clinically protected from GVHD as shown by a decreased weight loss, reduced clinical GVHD scores, and preserved colon lengths (Fig. 2a, b and Supplementary Fig. S2A−B). This attenuated clinical phenotype was further paralleled by reduced histological severity scores of the colon and the liver, the two major GVHD target organs (Fig. 2c and Supplementary Fig. S2C). Fk866-treated animals were protected from GVHD-induced disease even after prolonged administration (Supplementary Fig. S2D−G), whereas syngeneic groups were indistinguishable in any of the assessed parameters (Fig. 2a–c and Supplementary Fig. S2A−G). Furthermore, the achieved in vivo concentrations of Fk866 (as measured by mass spectrometry, Supplementary Fig. S2H) did not impair major peripheral blood parameters in syngeneic or allogeneic animals (Supplementary Fig. S2I). Notably, Fk866 treatment resulted in similar therapeutic efficacy after conditioning with either TBI or BU/CY, which are the standard myeloablative conditioning regimens in human allo-HSCT.

Fk866 induces apoptosis in effector T cells but spares regulatory and memory T cells

To determine whether the ameliorated phenotype after allo-BMT was a consequence of Fk866-mediated effects on different T-cell subsets, we analyzed splenic and colonic lymphocytes by flow cytometry. Early after BMT and as expected, allogeneic but not syngeneic transplantation resulted in a marked expansion of $CD8^+$ and $CD4^+$ T cells in the spleen as well as in the colon, a major target during GVHD (Fig. 3a, b). In contrast, Fk866 administration resulted in decreased frequencies of donor-derived $CD4^+$ and $CD8^+$ T cells at both sites. Moreover, Fk866 was accompanied by higher frequencies of $CD4^+$ $CD25^+$ $FoxP3^+$ regulatory T cells (Treg), although this was not

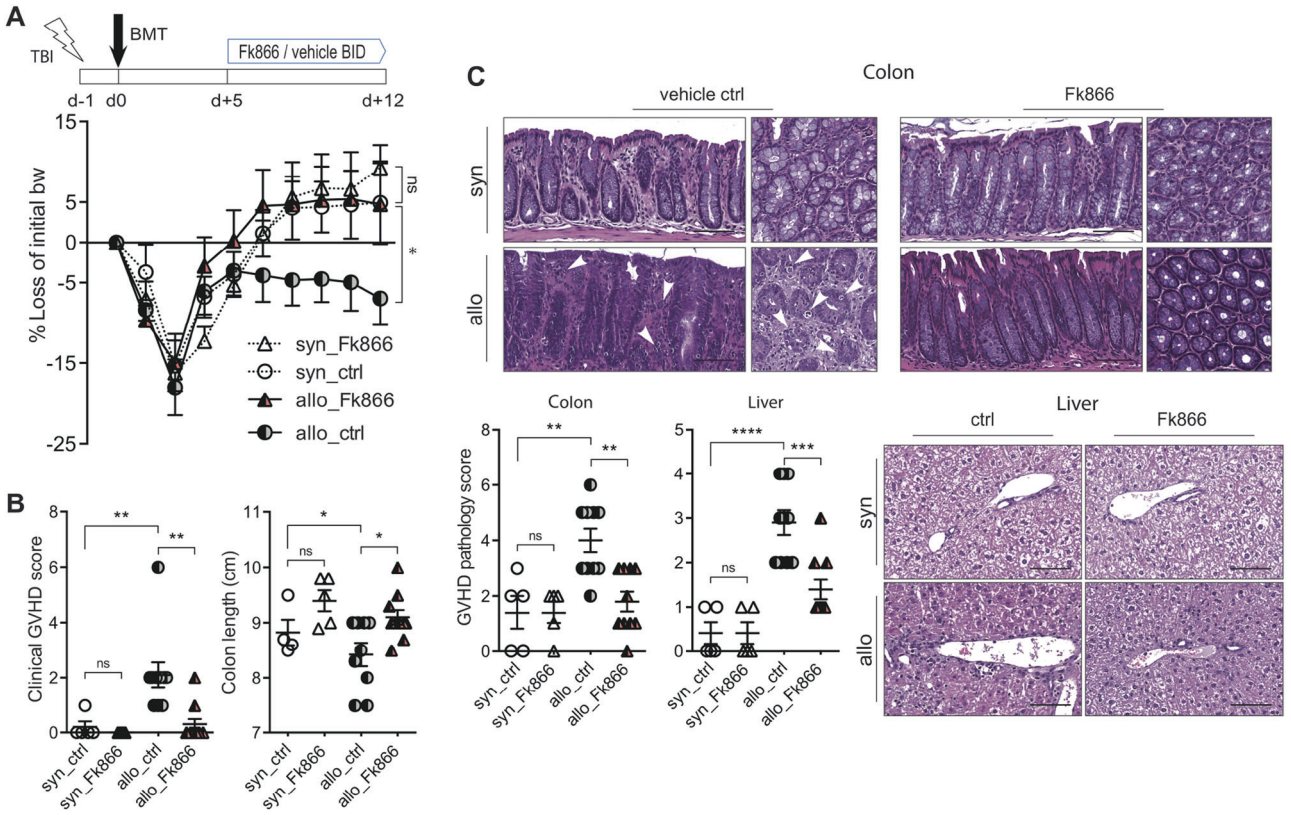

Fig. 2 Fk866-mediated Nampt inhibition mitigates acute GVHD in major mismatch models. B6 recipient mice were transplanted with 5×10^6 TCD bone marrow cells from B6 (syn) or BALB/c donors along with 1×10^6 T cells (allo). Mice were treated with Fk866 (6 mg/kg bw BID) or vehicle control from d +5 until the end of experiments (d + 12). **a** Experimental outline and weight course of respective groups are shown. **b** Graphs represent the clinical GVHD scores and colon lengths of mice at the end of experiments. **c** Histopathologic GVHD scores of colon and liver along with representative H&E stained sections of indicated groups are shown. White arrowheads indicate typical apoptotic crypt cells. (×20 magnification, scale bars represent 50 µm). $n = 4$ (syn), 10 (allo)/group; five independent experiments. Data represent mean ± SEM. $*p < 0.05$; $**p < 0.01$; $***p < 0.001$; $****p < 0.0001$; BID, twice daily administration, bw bodyweight, TBI total body irradiation, BMT bone marrow transplantation, TCD T-cell depletion.

statistically significant (Fig. 3a, b). However, the Fk866-mediated reduction of Teff along with increased frequencies of Treg translated into a decreased ratio of $CD8^+$:Treg and $CD4^+$:Treg in favor of increased Treg numbers in both compartments (Fig. 3a, b). Importantly, numbers of memory T cells (Tmem), which contribute to antipathogen immunity, were not impaired by prolonged Fk866 administration (Supplementary Fig. S3A). Furthermore, we did not observe significant differences in the abundance of monocytes, macrophages, dendritic cells, or natural killer cells, with the latter also representing important effector cells during GVL (Supplementary Fig. S3B). Since Fk866 reduced $CD4^+$ and $CD8^+$ lymphocyte abundances during allo-BMT but not during syngeneic BMT, we hypothesized that alloantigen-activated T lymphocytes are particularly susceptible to Nampt blockade. In subsequent experiments, animals were treated with vehicle or Fk866 for 48 h and analyzed for apoptotic T lymphocytes in spleens (gating strategies outlined in Supplementary Fig. S3C). Fk866 significantly increased apoptosis of $CD3^+$ T cells during aGVHD but not in the context of syngeneic BMT (Fig. 3c). These data indicate, that Fk866 selectively targets T cells during allogeneic activation while sparing Tmem and Treg.

T-cell subsets exhibit differential susceptibility to Fk866-induced NAD shortage

We next sought to investigate the role of Nampt and its blockage in T lymphocytes in vitro. $CD8^+$, $CD4^+$ $CD25^-$ (conventional T cells, i.e., Tcon) and $CD4^+$ $CD25^+$ (natural Treg, i.e., Treg) T cells were isolated from B6 mice and stimulated with anti-CD3/CD28. Whereas T-cell receptor (TCR) stimulation resulted in a more than 16- and 3-fold upregulation of Nampt mRNA in $CD8^+$ and $CD4^+$ T cells, respectively, its expression in Tregs was only modestly upregulated (1.3-fold, ns) compared with baseline (Fig. 4a). We next tested the susceptibility of these lymphocyte subsets to Fk866 and found, that $CD8^+$ and $CD4^+$ T cells displayed reduced viability upon Fk866 in a dose-dependent manner with the most pronounced effects on $CD8^+$ T cells

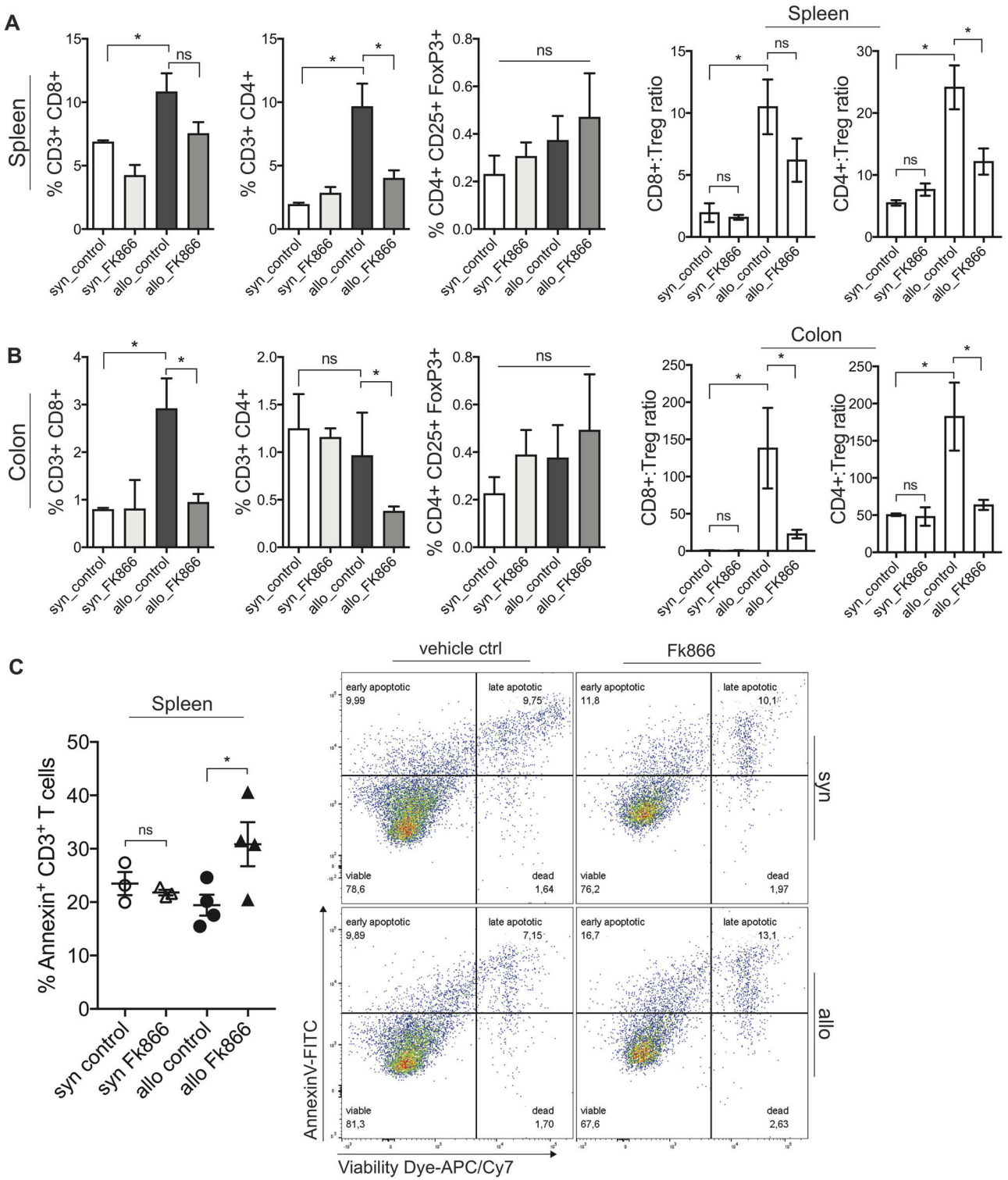

Fig. 3 Fk866 targets effector T cells and promotes regulatory T cells during acute GVHD. B6 mice underwent syngeneic or allogeneic BMT as depicted in Fig. 2a. On day +12, splenocytes (**a**) and LPMC (**b**) were isolated and analyzed by flow cytometry. Respective T-cell subsets are expressed as percentage out of the live $CD45^+$ population. The ratios of $CD4^+$ or $CD8^+$ T cells to Treg in spleens and colons were calculated by dividing total counts of respective cell subsets and normalized to $CD45^+$ cells. $n = 4$ (syn), 6 (allo)/ group; three independent experiments. **c** Experiments were performed as described in Fig. 2a and Fk866 or vehicle treatment was started on d +5. 48 h after treatment initiation (i.e., a total of four applications), spleens were assessed for apoptotic $CD3^+$ T cells by flow cytometry utilizing AnnexinV and viability staining. Graphs display the sum of early and late apoptotic splenic T cells ($AnnexinV^+$) along with representative dot plots of respective experimental groups. $n = 3$ (syn), 4 (allo) per group; two independent experiments. Data represent mean ± SEM. $^*p < 0.05$; $^{**}p < 0.01$; $^{***}p < 0.001$. LPMC lamina propria mononuclear cells, Treg regulatory T cells.

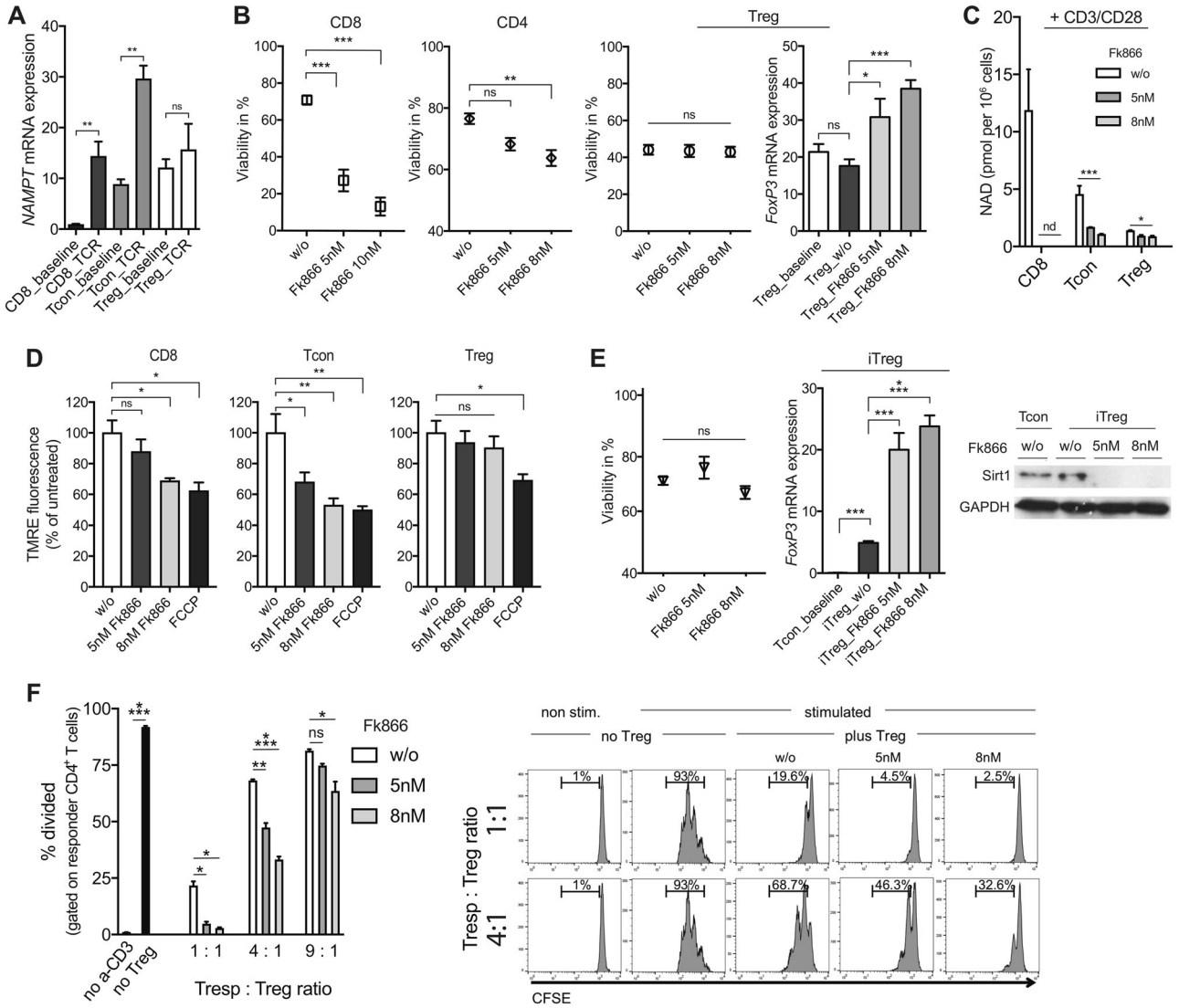

Fig. 4 NAD depletion differentially impacts T-cell subsets. a $CD8^+$, $CD4^+$ $CD25^-$ (Tcon) and $CD4^+$ $CD25^+$ (Tregs) T cells were freshly isolated from spleens of B6 mice and assessed for Nampt mRNA expression at baseline and after 24 h of CD3/CD28 stimulation (TCR). **b** $CD8^+$ T cells, Tcon, and Treg were cultured in the presence of CD3/CD28 and indicated doses of Fk866 for 48 or 72 (Tcon and Treg) hours. Cell viability was examined by PI staining. FoxP3 mRNA expression was quantified in Treg after 72 h. **c** Intracellular NAD levels of TCR-stimulated T-cell subsets treated with or without Fk866 for 24 h are shown. **d** For assessment of the mitochondrial membrane potential, T cells were cultured for 48 h as described above or treated with the ionophore uncoupler FCCP, followed by TMRE staining and analysis. **e** Tcon were cultured in the presence of CD3/CD28, IL−2, TGFβ, and indicated doses of Fk866 for 5d and assessed for cell viability and FoxP3 mRNA expression. Sirt1 abundance was quantified using immunoblot analysis. Pooled data from five independent experiments. **f** Fk866 or vehicle control pretreated iTregs were recovered from respective cultures and used for subsequent suppression assays. Freshly isolated Tcon responder cells were cultured in the presence of anti-CD3 (1 µg/ml) and mitomycin-treated APC cells alone or together with different ratios of respective iTreg as indicated. Bar graphs show Tcon proliferation as assessed by CFSE dilutions together with representative histograms of CFSE-stained Tcon responders. One representative out of three independent experiments is shown. Data represent mean ± SEM. $*p < 0.05$; $**p < 0.01$; $***p < 0.001$. TCR T-cell receptor stimulation, PI propidium iodide, Tcon conventional T cells, Treg regulatory T cells, APC antigen-presenting cells, IL Interleukin, IFNγ interferon γ, TNFα tumor necrosis factor α, FoxP3 forkhead box P3, TMRE tetramethyl rhodamine ethyl ester, TGFβ transforming growth factor β, Tresp T-cell responders, nd not detectable, FCCP carbonyl cyanide-4-phenylhydrazone, CFSE carboxyfluorescein succinimidyl ester.

(Fig. 4b). Furthermore, Fk866 strongly impaired mRNA expressions of the effector cytokines interferon gamma (IFNγ) and tumor necrosis factor alpha (TNFα) in both subsets (Supplementary Fig. S4A). In contrast, Fk866 treatment did not alter Treg viability, but instead resulted in a dose-dependent upregulation of the key Treg transcription factor forkhead box P3 (FoxP3) (Fig. 4b). Given that a balanced NAD/NADH ratio is a prerequisite for efficient cytoplasmic and mitochondrial metabolism and NAD depletion below a critical threshold triggers cell death [31],

we quantified intracellular NAD levels following Fk866 treatment. Consistent with the TCR-induced upregulation of Nampt (Fig. 4a), $CD8^+$ and $CD4^+$ T cells displayed higher total NAD levels compared with Treg, which were strongly depleted consequent to Fk866 treatment (Fig. 4c). These observations were paralleled by a significantly decreased mitochondrial transmembrane potential already after 48 h in Teff but not in Treg cells (Fig. 4d).

FoxP3 expression in Tregs is controlled on multiple layers and involves the concerted action of other transcription factors, epigenetic mechanisms and posttranscriptional regulation [32]. To further elucidate, how Fk866-mediated NAD depletion promoted Tregs, we investigated potential molecular regulators of FoxP3 and found, that the protein levels of the NAD-dependent HDAC Sirt1 were strongly reduced in Treg cells upon treatment (Supplementary Fig. S4B). To assess, whether NAD limitation would impact Treg development, we cultured Tcon under Treg-inducing conditions (i.e., iTreg) with or without Fk866 and performed quantitative and qualitative evaluation of the cells. Consistent with the observations in natural Treg cells, presence of Fk866 did not impair viability and resulted in a dose-dependent reduction of Sirt1, which was accompanied by increased FoxP3 mRNA expression and protein (Fig. 4e and Supplementary Fig. S4C). In subsequent suppression assays, Fk866-pretreated iTreg revealed markedly increased suppressive capacity in comparison to vehicle-treated iTreg cells (Fig. 4f).

Fk866 exerts potent antitumor efficacy without enhancing the risk of leukemic relapse in experimental GVL

GVHD and GVL are tightly linked processes and suppressing GVHD without compromising the GVL effect remains a major therapeutic challenge. Since Fk866 was beneficial in experimental GVHD by suppressing Teff and promoting Treg, we next sought to investigate its net consequence in common GVL models. Mice underwent syngeneic or allogeneic BMT along with inoculation of myelomonocytic leukemia cells (WEHI-3B *luc*) followed by T-cell transfer in the allo-BMT group. Fk866 or vehicle control treatment was started on d +5 (outlined in Fig. 5a) and mice were subjected to BLI on d +12. As expected, animals receiving syngeneic BM and WEHI-3B rapidly developed leukemia with infiltration of BM, liver, and spleen (Fig. 5b). In marked contrast, Fk866-treated mice demonstrated strongly reduced tumor engraftment/leukemia as illustrated by BLI (Fig. 5b, c), suggesting a direct antitumor effect. Compared with syngeneic animals, allo-BMT resulted in a decreased tumor burden in vehicle-treated animals (Fig. 5b, c) but was accompanied by severe clinical and histological signs of GVHD (Fig. 5d, e). However, Fk866 treatment significantly abrogated these GVHD attributes but simultaneously suppressed tumor growth (Fig. 5b–e). These findings were corroborated by in vitro experiments, exposing WEHI-3B cells to increasing Fk866 doses, followed by NAD quantification and BLI. Compared with control-treated cells, intracellular NAD dropped in a dose-dependent manner, which was paralleled by reduced proliferation visualized by bioluminescence (Fig. 5f). In a second set of experiments, we investigated Fk866's antiproliferative capacity on the murine B cell lymphoma cell line A20. In line with our findings from the WEHI-GVL model, Fk866-treated animals were highly protected from tumor cell expansion in both, the syngeneic and the allogeneic setting (Supplementary Fig. 5B). Simultaneously, GVHD-associated parameters including weight loss, colonic shortening, as well as clinical and histopathological GVHD severity were strongly ameliorated (Supplementary Fig. 5A, C–E). Likewise, Fk866 inhibited proliferation of cultured A20 in a dose-dependent manner as assessed by BLI (Supplementary Fig. 5F). Collectively, these data suggest, that Fk866 mediates a potent antitumor effect onto murine leukemia and lymphoma cells while simultaneously ameliorating GVHD.

Fk866 suppresses human T-cell proliferation and promotes regulatory T cells ex vivo

To substantiate our findings in mice, we first investigated the antiproliferative capacity of Fk866 on PBMC from healthy human donors in vitro. Following different TCR stimulations, leukocytes were cultured in the presence or absence of the standard immunosuppressants CsA and dexamethasone (DXA) and compared with Fk866. As expected, CsA and DXA dose-dependently inhibited T-cell proliferation after PHA- and CD3/CD28 stimulation and were effective in a one-way mixed lymphocyte reaction (Fig. 6a). Fk866 showed comparable suppressive activity as determined by the ^{3}H-thymidine incorporation method (Fig. 6a). Since Fk866-mediated NAD depletion also affected the biology of murine Tregs, we wondered if this observation could be recapitulated in human iTreg cells. Naive $CD4^+$ T cells were differentiated towards FoxP3-expressing iTreg cells in the presence or absence of Fk866. In agreement with our findings in mice, Nampt inhibition resulted in increased FoxP3 and decreased SIRT1 mRNA expression (Fig. 6b). Finally, we tested Fk866 on PBMC from treatment−naive patients diagnosed with grade II−IV aGVHD. After PHA stimulation, cells were incubated with DXA or Fk866 followed by ^{3}H−thymidine incorporation assays. Again, Fk866 dose-dependently suppressed cell proliferation, whereas DXA was only effective at higher doses (Fig. 6c and Supplementary Fig. S6A).

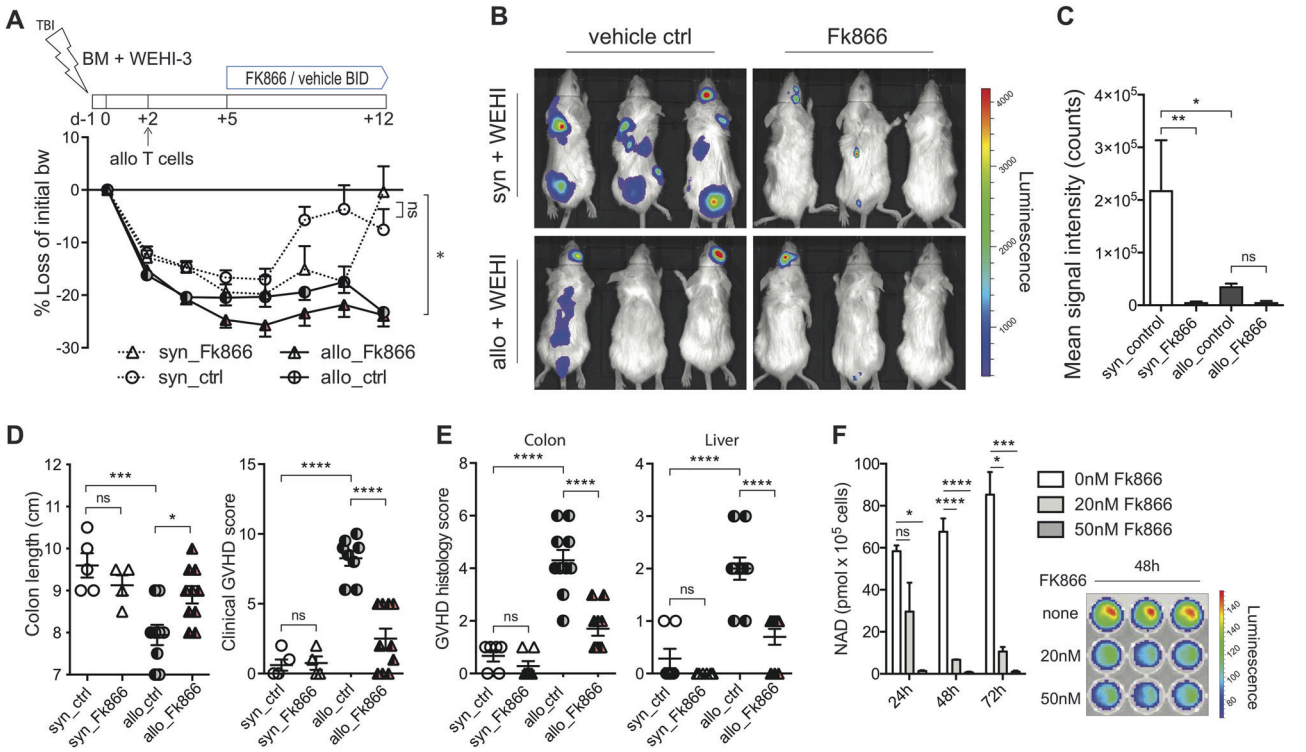

Fig. 5 Tumor cells are highly susceptible to Fk866 in experimental leukemia and GVL models. (**a**) Experimental design and weight course of the GVL model are shown. BALB/c mice received 5×10^6 TCD BM cells from BALB/c (syn) or B6 donors (allo) along with 1×10^6 WEHI-3B *luc* on day 1 followed by injection of 0.5×10^6 splenic T cells (B6) of respective groups 48 h thereafter. Fk866 or vehicle treatment was started on day 5. **b** Tumor localization in respective experimental groups together with (**c**) total tumor burden as assessed by BLI on day 12 is shown. $n = 4$ for syngeneic groups, $n = 9$ for allo-ctr., $n = 10$ for allo–Fk866; three independent experiments. **d** Graphs represent colon lengths and clinical GVHD scores of mice at the end of experiments together with (**e**) histopathological analysis of colon and liver. $n = 4$ (syn), 10 (allo) per group, one representative out of three independent experiments is shown. Data represent mean ± SEM. **f** Intracellular NAD levels of WEHI-3B cells with and without Fk866 were assessed over time and corroborated by cell expansion studies utilizing bioluminescence imaging. $*p < 0.05$; $**p < 0.01$; $***p < 0.001$; $****p < 0.0001$. GVL graft-versus-leukemia, TCD T-cell depletion, BM bone marrow.

Discussion

The extraordinary metabolic requirements of rapidly proliferating cells have recently received considerable attention as therapeutic targets in cancer, inflammation/autoimmunity, and transplant biology [12, 13, 33–35]. Herein, we provide evidence, that Nampt and the NAD immunometabolism are implicated in experimental and human aGVHD, which can be therapeutically exploited by the small-molecule inhibitor Fk866.

Nampt is a pleiotropic protein with heterogenous functions and we propose, that the increased circulating NAMPT levels in patients with established GVHD result from a combination of common phenomena. First, activated immune cells have been shown to secrete Nampt in a cytokine-like manner, resulting in the induction of other proinflammatory mediators including TNFα [10, 36, 37]. Other reports suggest, that extracellular Nampt simply represents intracellular protein, which is extracellularly released rather than secreted upon activation-induced cell death of immune cells, similarly to necrotic/apoptotic cells in inflamed tissues [21]. In our study, GVHD patients displayed highly elevated NAMPT serum levels, which peaked around the mean clinical disease onset. Interestingly, NAMPT was already increased prior to allo−BMT, which might identify patients with an a priori proinflammatory state. However, whether increased pre-transplant NAMPT entails higher susceptibility towards or triggers clinically relevant GVHD, and if NAMPT serves as valid biomarker remains to be investigated. Notably, NAMPT upregulation in conjunctival epithelial cells has been associated with ocular GVHD [38].

The proinflammatory cytokine cascade during GVHD plays a central role in disease initiation and perpetuation, likely further enhancing Nampt upregulation and vice-versa. The GI-tract is particularly susceptible to damage from proinflammatory cytokines like TNFα but is itself a critical amplifier of systemic GVHD [39]. Our data show, that Fk866 markedly decreased intestinal and hepatic pathologies in several experimental GVHD models, resulting in reduced disease parameters. Despite the potent

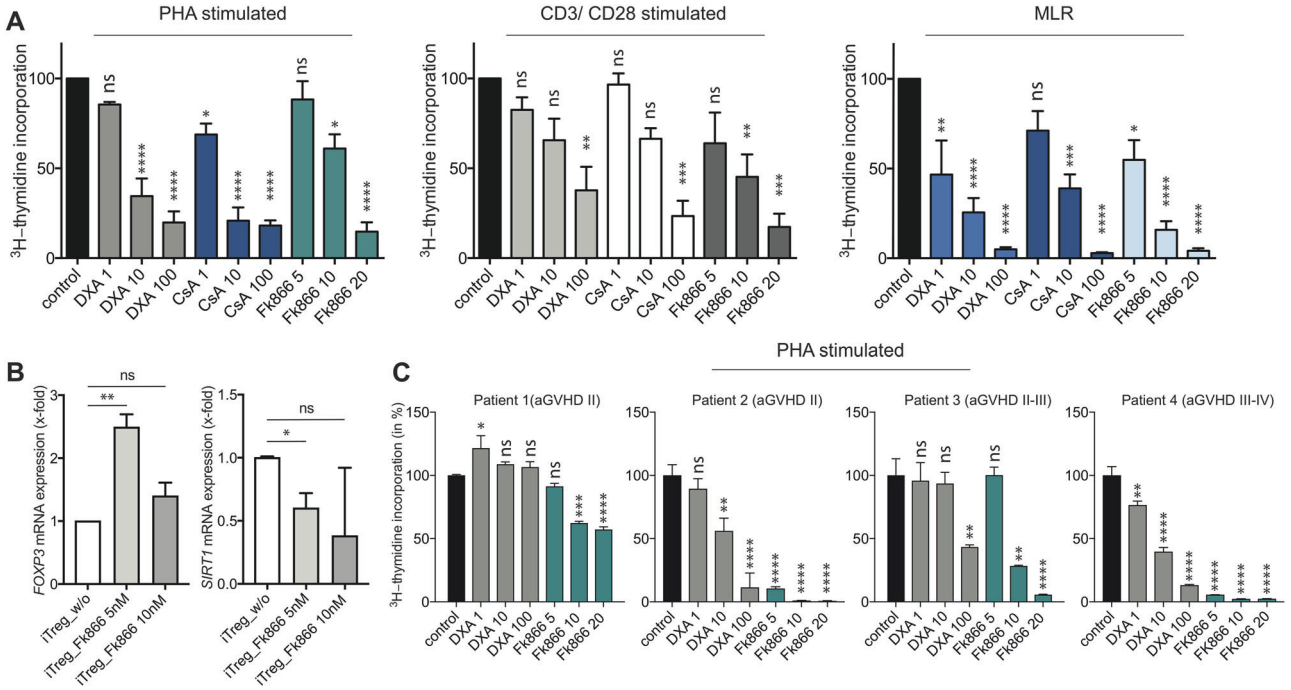

Fig. 6 Fk866 suppresses lymphocyte proliferation from healthy and GVHD patients and promotes iTreg. a PBMCs from healthy volunteers were stimulated with PHA, CD3/CD28 or used in a one-way MLR and incubated in the presence or absence of dexamethasone (DXA, 1–100 nM), cyclosporine A (CsA, 1–100 ng/ml) or Fk866 (5–20 nM). Proliferation was assessed by the ^{3}H-thymidine incorporation method. **b** Human CD4^{+} T cells from healthy volunteers were differentiated towards iTreg cells in the presence or absence of Fk866 and assessed for FOXP3 and SIRT1 mRNA expression on day 5 of culture. $n = 4$. **c** PBMCs from treatment−naive GVHD patients were stimulated with PHA and incubated with respective compounds as described in (**a**). $n = 4$. A grouped data display is shown in Supplementary Fig. S6. Data represent mean ± SEM. *$p < 0.05$; **$p < 0.01$; ***$p < 0.001$; ****$p < 0.0001$. PBMCs peripheral blood mononuclear cells, PHA phytohemagglutinin A, MLR mixed lymphocyte reaction.

suppressive effect onto alloantigen-activated Teff, the frequencies of Treg and Tmem remained unaffected, even after prolonged Fk866 application. This might be at least partly explained by the differing metabolic demands and signatures of specific T-cell subsets [2]. While Treg and Tmem tend to engage mitochondrial oxidative phosphorylation and lipid oxidation, Teff preferentially produce ATP in a Warburg-like manner [7, 20, 21, 40, 41]. The latter is also critical for T-cell proliferation and effector functions during allogeneic responses [22]. Previous studies demonstrated, that Fk866 treatment impairs various processes including glycolysis, resulting in further disruption of downstream metabolic pathways, and, if NAD levels reach a critical threshold, trigger cell death [31, 42, 43]. Along these lines, intestinal T cells during human and mouse GVHD and in vitro activated Teff cells strongly upregulated Nampt, which likely explains why these cells were particularly susceptible to Fk866-induced NAD depletion. Fk866 treatment resulted in a disrupted mitochondrial membrane potential in Teff, which was not observed in Tregs. These data suggest that the differential metabolic demands of Teff versus Treg and Tmem offer a therapeutic window to inhibit alloantigen-activated Teff proliferation without conferring a generalized immunosuppression.

Besides its role in energy metabolism, NAD availability is essential for protein acetylation/deacetylation mediated by sirtuins and other HDACs, thereby contributing to epigenetic regulation [44]. As a consequence, NAD depletion results in suppression of such enzymes, which represents another important target mechanism of Fk866 [13, 45]. Several studies demonstrated that Sirt1-mediated deacetylation regulates FoxP3 levels, which has been linked to enhanced allograft survival and reduced GVHD development, similar to observations with HDAC inhibitors [46–49]. In our study, Fk866 treatment resulted in a robust increase in FoxP3 levels and a concomitant reduction of Sirt1 expression, which was associated with enhanced suppressive properties of iTregs. Although Fk866 did not significantly expand Treg frequencies in vivo, increased FoxP3 expression promotes Treg stability and furthermore confers a metabolic advantage, which is required and sufficient for Treg lineage commitment and suppressor function [49, 50]. This might partly explain, why Fk866-challenged Tregs were resistant to NAD deprivation, which adds a novel attribute to Fk866's mode of actions.

In the context of tumor immunity, T cell depleting strategies and increased Treg abundance or function have been linked to higher relapse rates and poor clinical

prognosis [51, 52]. The most attractive incentive for utilizing Fk866 in the treatment of aGVHD is highlighted by the remarkable metabolic similarities of activated lymphocytes and cancer cells. In addition to effectively controlling GVHD, Fk866 revealed potent antitumor properties in experimental leukemia/B cell lymphoma and GVHD/GVL models without increasing leukemic relapse. This is in accordance with previous reports, demonstrating that various cancer entities including hematologic malignancies are highly susceptible to Nampt blockage [14, 45, 53].

The data presented herein may have important clinical relevance. CsA as the backbone of GVHD prophylaxis and corticosteroids as the first-line therapy frequently fail to prevent or resolve GVHD and moreover, CsA has been shown to negatively impact Treg function [19, 54–56]. In ex vivo approaches, those compounds equally suppressed lymphocyte proliferation from healthy donors. However, Fk866 showed superior efficacy on PBMCs from treatment–naive GVHD patients compared with dexamethasone. Steroids confer a nonspecific long term immunosuppression and are associated with significant toxicities including GI adverse events and infectious complications [57]. The available treatment options particularly for GI−GVHD remain unsatisfactory in the clinical setting and steroid-refractory patients have a poor prognosis regardless of the utilized salvage treatment [58]. In our study, Fk866-treated mice were highly protected from GI and hepatic GVHD, without a generalized immunosuppression. This is also supported by the absence of any obvious effects in the syngeneic setting such as peripheral hematopoietic reconstitution, the composition of various immune cell subsets, weight course and histology. So far, Fk866 has been investigated for its antineoplastic properties in clinical trials, mainly based on the hypothesis that NAD depletion would result in consequent ATP depletion and irreversible cell death of cancer cells [59, 60]. These studies revealed reasonable toxicity and importantly, Fk866 can be effectively antagonized by its antidote nicotinic acid/vitamin B_3, thus providing a potential therapeutic alternative to steroids. Considering our data demonstrating increased NAMPT levels in GVHD patients, this might ultimately identify patients who benefit from Fk866-mediated NAMPT blockade towards a more targeted pharmacological approach that warrants further investigations.

In conclusion, Nampt blockage might display a metabolic checkpoint, achieving reasonable cellular selectivity based on the context of its employment. Thus, blocking NAD metabolism represents a promising approach to simultaneously target alloreactive T cells and cancer cells while preserving regulatory and memory T cells during aGVHD.

Acknowledgements We thank Alexandra Pfister, Christina Schwabegger, Barbara Enrich, Heide Dierbach, Alexandra Wegmayr, and Werner Klotz for excellent technical assistance and helpful advice. We thank H.G. Knaus for generously allocating lab space and the team of the University Hospital for Radiotherapy and Radiation Oncology for providing irradiation equipment. This study was supported by the intramural funding program of the Medical University Innsbruck for young scientists MUI−START (project 2016−01−006 to RRG) and by the Austrian Society of Gastroenterology and Hepatology (ÖGGH to RRG). HT was supported by the Austrian Research Promotion Agency FFG (K−Project No. 843536) funded by the BMVIT, BMWFW, the Wirtschaftsagentur Wien and the Standortagentur Tirol.

Author contributions RRG, SM, KS, FG, LM, BT and BK performed experiments. SR and KS performed flow cytometry analysis. PM provided pathology expertise. ME, HS, ARM and DN provided access to clinical samples and HO performed LC−MS/MS studies. ARM, HT, RZ and DN provided critical feedback and contributed to paper preparation. RRG conceived the study, analyzed and interpreted data and prepared the paper together with SM and DN.

Compliance with ethical standards

Conflict of interest The authors declare that they have no conflict of interest.

Publisher's note Springer Nature remains neutral with regard to jurisdictional claims in published maps and institutional affiliations.

References

1. Olenchock BA, Rathmell JC, Heiden MGV. Biochemical underpinnings of immune cell metabolic phenotypes. Immunity 2017; 46:703–13.
2. Fox CJ, Hammerman PS, Thompson CB. Fuel feeds function: energy metabolism and the T-cell response. Nat Rev Immunol. 2005;5:844–52.
3. Vander Heiden MG, Cantley LC, Thompson CB. Understanding the Warburg effect: the metabolic requirements of cell proliferation. Science. 2009;324:1029–33.
4. Nikiforov A, Kulikova V, Ziegler M. The human NAD metabolome: functions, metabolism and compartmentalization. Crit Rev Biochem Mol Biol. 2015;50:284–97.
5. Michan S, Sinclair D. Sirtuins in mammals: insights into their biological function. Biochem J. 2007;404:1–13.
6. Wang T, Zhang X, Bheda P, Revollo JR, Imai S, Wolberger C. Structure of Nampt/PBEF/visfatin, a mammalian NAD+ biosynthetic enzyme. Nat Struct Mol Biol. 2006;13:661–2.
7. Moschen AR, Kaser A, Enrich B, Mosheimer B, Theurl M, Niederegger H, et al. Visfatin, an adipocytokine with proinflammatory and immunomodulating properties. J Immunol. 2007; 178:1748–58.
8. Li Y, Zhang Y, Dorweiler B, Cui D, Wang T, Woo CW, et al. Extracellular Nampt promotes macrophage survival via a nonenzymatic interleukin-6/STAT3 signaling mechanism. J Biol Chem. 2008;283:34833–43.
9. Jieyu H, Chao T, Mengjun L, Shalong W, Xiaomei G, Jianfeng L, et al. Nampt/Visfatin/PBEF: a functionally multi-faceted protein with a pivotal role in malignant tumors. Curr Pharm Des. 2012;18: 6123–32.
10. Moschen AR, Gerner RR, Tilg H. Pre-B cell colony enhancing factor/NAMPT/visfatin in inflammation and obesity-related disorders. Curr Pharm Des. 2010;16:1913–20.
11. Garten A, Petzold S, Korner A, Imai S, Kiess W. Nampt: linking NAD biology, metabolism and cancer. Trends Endocrinol Metab. 2009;20:130–8.

12. Hasmann M, Schemainda I. FK866, a highly specific noncompetitive inhibitor of nicotinamide phosphoribosyltransferase, represents a novel mechanism for induction of tumor cell apoptosis. Cancer Res. 2003;63:7436–42.
13. Gerner RR, Klepsch V, Macheiner S, Arnhard K, Adolph TE, Grander C, et al. NAD metabolism fuels human and mouse intestinal inflammation. Gut. 2018;67:1813–23.
14. Nahimana A, Attinger A, Aubry D, Greaney P, Ireson C, Thougaard AV, et al. The NAD biosynthesis inhibitor APO866 has potent antitumor activity against hematologic malignancies. Blood. 2009;113:3276–86.
15. Zeiser R, Blazar BR. Acute graft-versus-host disease—biologic process, prevention, and therapy. N. Engl J Med. 2017;377:2167–79.
16. Hill GR, Ferrara JL. The primacy of the gastrointestinal tract as a target organ of acute graft-versus-host disease: rationale for the use of cytokine shields in allogeneic bone marrow transplantation. Blood. 2000;95:2754–9.
17. Weisdorf D, Haake R, Blazar B, Miller W, McGlave P, Ramsay N, et al. Treatment of moderate/severe acute graft-versus-host disease after allogeneic bone marrow transplantation: an analysis of clinical risk features and outcome. Blood. 1990;75:1024–30.
18. Roy J, McGlave PB, Filipovich AH, Miller WJ, Blazar BR, Ramsay NK, et al. Acute graft-versus-host disease following unrelated donor marrow transplantation: failure of conventional therapy. Bone Marrow Transpl. 1992;10:77–82.
19. Westin JR, Saliba RM, De Lima M, Alousi A, Hosing C, Qazilbash MH, et al. Steroid-refractory acute GVHD: predictors and outcomes. Adv Hematol. 2011;2011:601953.
20. Bruzzone S, Fruscione F, Morando S, Ferrando T, Poggi A, Garuti A, et al. Catastrophic NAD+ depletion in activated T lymphocytes through Nampt inhibition reduces demyelination and disability in EAE. PLoS One. 2009;4:e7897.
21. Rongvaux A, Shea RJ, Mulks MH, Gigot D, Urbain J, Leo O, et al. Pre-B-cell colony-enhancing factor, whose expression is upregulated in activated lymphocytes, is a nicotinamide phosphoribosyltransferase, a cytosolic enzyme involved in NAD biosynthesis. Eur J Immunol. 2002;32:3225–34.
22. Nguyen HD, Chatterjee S, Haarberg KM, Wu Y, Bastian D, Heinrichs J, et al. Metabolic reprogramming of alloantigen-activated T cells after hematopoietic cell transplantation. J Clin Investig. 2016;126:1337–52.
23. Storb R, Deeg HJ, Whitehead J, Appelbaum F, Beatty P, Bensinger W, et al. Methotrexate and cyclosporine compared with cyclosporine alone for prophylaxis of acute graft versus host disease after marrow transplantation for leukemia. N. Engl J Med. 1986;314:729–35.
24. McSweeney PA, Niederwieser D, Shizuru JA, Sandmaier BM, Molina AJ, Maloney DG, et al. Hematopoietic cell transplantation in older patients with hematologic malignancies: replacing high-dose cytotoxic therapy with graft-versus-tumor effects. Blood. 2001;97:3390–400.
25. Przepiorka D, Weisdorf D, Martin P, Klingemann HG, Beatty P, Hows J, et al. Consensus conference on acute Gvhd grading. Bone Marrow Transpl. 1995;15:825–8.
26. Zeiser R, Leveson-Gower DB, Zambricki EA, Kambham N, Beilhack A, Loh J, et al. Differential impact of mammalian target of rapamycin inhibition on CD4+CD25+Foxp3+ regulatory T cells compared with conventional CD4+ T cells. Blood. 2008;111:453–62.
27. Cooke KR, Kobzik L, Martin TR, Brewer J, Delmonte J Jr, Crawford JM, et al. An experimental model of idiopathic pneumonia syndrome after bone marrow transplantation: I. The roles of minor H antigens and endotoxin. Blood. 1996;88:3230–9.
28. Glass B, Uharek L, Zeis M, Loeffler H, MuellerRuchholtz W, Gassmann W. Graft-versus-leukaemia activity can be predicted by natural cytotoxicity against leukaemia. Brit J Haematol. 1996;93:412–20.
29. Zeiser R, Youssef S, Baker J, Kambham N, Steinman L, Negrin RS. Preemptive HMG-CoA reductase inhibition provides graft-versus-host disease protection by Th-2 polarization while sparing graft-versus-leukemia activity. Blood. 2007;110:4588–98.
30. Edinger M, Cao YA, Verneris MR, Bachmann MH, Contag CH, Negrin RS. Revealing lymphoma growth and the efficacy of immune cell therapies using in vivo bioluminescence imaging. Blood. 2003;101:640–8.
31. Del Nagro C, Xiao Y, Rangell L, Reichelt M, O'Brien T. Depletion of the central metabolite NAD leads to oncosis-mediated cell death. J Biol Chem. 2014;289:35182–92.
32. Lu L, Barbi J, Pan F. The regulation of immune tolerance by FOXP3. Nat Rev Immunol. 2017;17:703–17.
33. Gatza E, Wahl DR, Opipari AW, Sundberg TB, Reddy P, Liu C, et al. Manipulating the bioenergetics of alloreactive T cells causes their selective apoptosis and arrests graft-versus-host disease. Sci Transl Med. 2011;3:67ra8.
34. Lee CF, Lo YC, Cheng CH, Furtmuller GJ, Oh B, Andrade-Oliveira V, et al. Preventing allograft rejection by targeting immune metabolism. Cell Rep. 2015;13:760–70.
35. Molina JR, Sun YT, Protopopova M, Gera S, Bandi M, Bristow C, et al. An inhibitor of oxidative phosphorylation exploits cancer vulnerability. Nat Med. 2018;24:1036–46.
36. Grolla AA, Travelli C, Genazzani AA, Sethi JK. Extracellular nicotinamide phosphoribosyltransferase, a new cancer metabokine. Br J Pharm. 2016;173:2182–94.
37. Samal B, Sun Y, Stearns G, Xie C, Suggs S, McNiece I. Cloning and characterization of the cDNA encoding a novel human pre-B-cell colony-enhancing factor. Mol Cell Biol. 1994;14:1431–7.
38. Cocho L, Fernandez I, Calonge M, Martinez V, Gonzalez-Garcia MJ, Caballero D, et al. Gene expression-based predictive models of graft versus host disease-associated dry eye. Investig Ophthalmol Vis Sci. 2015;56:4570–81.
39. Ferrara JL, Levine JE, Reddy P, Holler E. Graft-versus-host disease. Lancet. 2009;373:1550–61.
40. Pearce EL, Poffenberger MC, Chang CH, Jones RG. Fueling immunity: insights into metabolism and lymphocyte function. Science. 2013;342:1242454.
41. Newton R, Priyadharshini B, Turka LA. Immunometabolism of regulatory T cells. Nat Immunol. 2016;17:618–25.
42. Yang H, Yang T, Baur JA, Perez E, Matsui T, Carmona JJ, et al. Nutrient-sensitive mitochondrial NAD+ levels dictate cell survival. Cell. 2007;130:1095–107.
43. Tan B, Young DA, Lu ZH, Wang T, Meier TI, Shepard RL, et al. Pharmacological inhibition of nicotinamide phosphoribosyltransferase (NAMPT), an enzyme essential for NAD+ biosynthesis, in human cancer cells: metabolic basis and potential clinical implications. J Biol Chem. 2013;288:3500–11.
44. Wellen KE, Thompson CB. A two-way street: reciprocal regulation of metabolism and signalling. Nat Rev Mol Cell Biol. 2012;13:270–6.
45. Sampath D, Zabka TS, Misner DL, O'Brien T, Dragovich PS. Inhibition of nicotinamide phosphoribosyltransferase (NAMPT) as a therapeutic strategy in cancer. Pharm Therapeut. 2015;151:16–31.
46. van Loosdregt J, Vercoulen Y, Guichelaar T, Gent YYJ, Beekman JM, van Beekum O, et al. Regulation of Treg functionality by acetylation-mediated Foxp3 protein stabilization. Blood. 2010;115:965–74.
47. Beier UH, Wang L, Bhatti TR, Liu Y, Han R, Ge G, et al. Sirtuin-1 targeting enhances T regulatory (Treg) cell suppressive function by increasing Foxp3 and heat shock protein-70 expression and

promotes treg-dependent cardiac allograft survival. Am J Transpl. 2011;11:155-.
48. Choi S, Reddy P. HDAC inhibition and graft versus host disease. Mol Med. 2011;17:404–16.
49. Daenthanasanmak A, Iamsawat S, Chakraborty P, Nguyen HD, Bastian D, Liu C, et al. Targeting Sirt-1 controls GVHD by inhibiting T-cell allo-response and promoting Treg stability in mice. Blood. 2019;133:266–79.
50. Josefowicz SZ, Rudensky A. Control of regulatory T cell lineage commitment and maintenance. Immunity. 2009;30:616–25.
51. Nishikawa H, Sakaguchi S. Regulatory T cells in tumor immunity. Int J Cancer. 2010;127:759–67.
52. Saad A, Lamb LS. Ex vivo T-cell depletion in allogeneic hematopoietic stem cell transplant: past, present and future. Bone Marrow Transpl. 2017;52:1241–8.
53. Gehrke I, Bouchard ED, Beiggi S, Poeppl AG, Johnston JB, Gibson SB, et al. On-target effect of FK866, a nicotinamide phosphoribosyl transferase inhibitor, by apoptosis-mediated death in chronic lymphocytic leukemia cells. Clin Cancer Res. 2014;20:4861–72.
54. Yee GC, Self SG, McGuire TR, Carlin J, Sanders JE, Deeg HJ. Serum cyclosporine concentration and risk of acute graft-versus-host disease after allogeneic marrow transplantation. N. Engl J Med. 1988;319:65–70.
55. Ratanatharathorn V, Nash RA, Przepiorka D, Devine SM, Klein JL, Weisdorf D, et al. Phase III study comparing methotrexate and tacrolimus (prograf, FK506) with methotrexate and cyclosporine for graft-versus-host disease prophylaxis after HLA-identical sibling bone marrow transplantation. Blood. 1998;92:2303–14.
56. Zeiser R, Nguyen VH, Beilhack A, Buess M, Schulz S, Baker J, et al. Inhibition of CD4+CD25+ regulatory T-cell function by calcineurin-dependent interleukin-2 production. Blood. 2006;108:390–9.
57. Messer J, Reitman D, Sacks HS, Smith H, Chalmers TC. Association of adrenocorticosteroid therapy and peptic-ulcer disease. N. Engl J Med. 1983;309:21–4.
58. Levine JE, Logan B, Wu J, Alousi AM, Ho V, Bolanos-Meade J, et al. Graft-versus-host disease treatment: predictors of survival. Biol Blood Marrow Transpl. 2010;16:1693–9.
59. Holen K, Saltz LB, Hollywood E, Burk K, Hanauske AR. The pharmacokinetics, toxicities, and biologic effects of FK866, a nicotinamide adenine dinucleotide biosynthesis inhibitor. Investig New Drugs. 2008;26:45–51.
60. Goldinger SM, Gobbi Bischof S, Fink-Puches R, Klemke CD, Dreno B, Bagot M, et al. Efficacy and safety of APO866 in patients with refractory or relapsed cutaneous T-cell lymphoma: a phase 2 clinical trial. JAMA Dermatol. 2016;152:837–9.